2024_“ShuWei Cup”

Problem C：Modeling of pulsar timing noise deduction and atmospheric time delay deduction of time signals

Pulsars are rapidly rotating neutron stars with continuous and stable rotation, earning them the nickname "lighthouses of the universe." The spatial observation of pulsars plays a crucial role in deep space spacecraft navigation and the maintenance of time standards.

The application of pulsar time in atomic timekeeping is expected to improve the stability and reliability of local atomic clocks, representing a long-term direction for the future development of timekeeping. One of the key challenges in pulsar time research is how to solve the problem of reduced accuracy and stability due to pulsar timing noise.

Pulsar timing noise is a continuous disturbance that occurs over a long timescale (typically months or years) in the pulsar's rotation parameters. It manifests as the discrepancy between the predicted pulse arrival time (PT) and the actual arrival time (PT-TT), which never equals zero. Timing noise is generally "red noise" and is present in almost all pulsars, including millisecond pulsars. Some exhibit random variations, while others show quasi-periodicity, as shown in Figure 1.

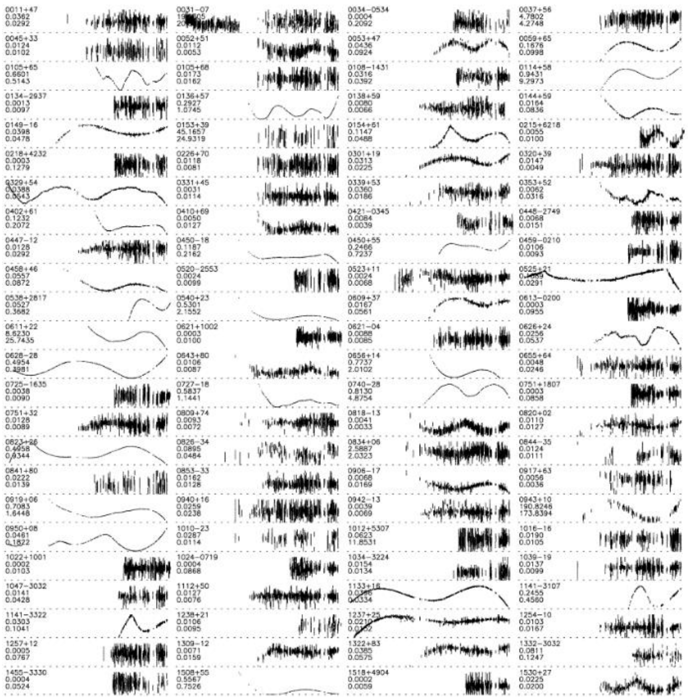

Figure 1: Timing noise chart of 96 pulsars (including millisecond pulsars) (Hobbs, 2010)

Pulsar timing noise primarily includes red noise from the pulsar's rotation, noise caused by dispersion measure (DM) variations, observational equipment noise, and noise at a specific frequency band. Data released by IPTA describe the red noise intensity using a power spectrum model as follows:

$$P(f) = \frac{P_0}{(1 + f^2 / f_c^2)^{q/2}}$$

Where P_0 represents the intensity of red noise, f is the Fourier frequency, f_c is the corner frequency, and q is the spectral index. In addition to the power spectrum estimation method (Matsakisd, 1997), methods used for pulsar timing noise estimation include Δ_8 models (Arzoumannian, 1994; Yang Tinggao, 2014), exponential models (Shannon, 2010), $\sigma_z(\tau)$ estimations (Reardon, 2016), and empirical mode decomposition (EMD) methods (Huang, 1998; Gao Feng, 2018). However, these methods can only improve the accuracy of pulsar models to a certain extent. The sources of pulsar timing noise are widespread and complex, making it a challenge to find effective methods for its handling. It remains an important task in PTA research. Some scholars have even attempted to use artificial intelligence methods to extract and model the features of timing noise (Liang Hongtao, 2023), aiming for better solutions in timing noise removal and prediction.

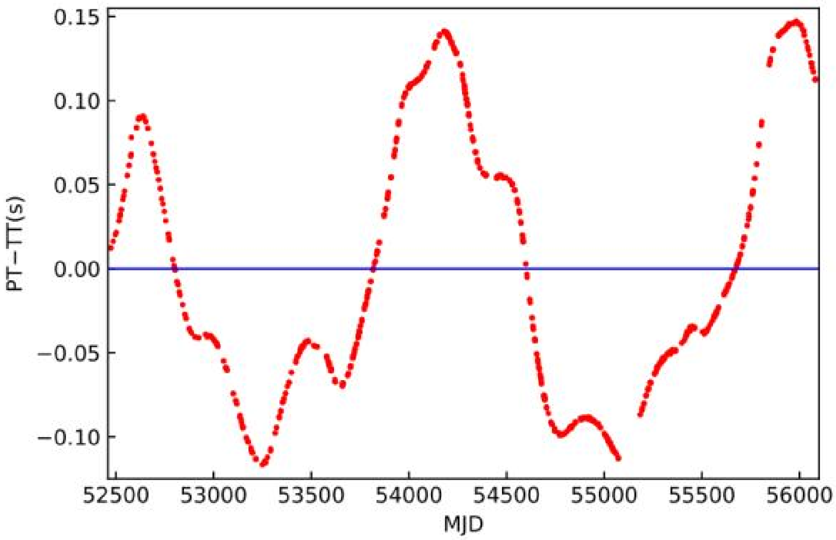

Figure 2: Pulsar timing noise of a particular pulsar

Pulsar time can create an independent time scale from atomic time and provide rich navigation information, such as position, velocity, and time, for spacecraft in low Earth orbit, geosynchronous orbit, highly elliptical Earth orbit, lunar orbit, interstellar navigation, and deep space navigation. The primary consideration in pulsar time is the pulse arrival time (TOA), which is influenced by various delay effects. Therefore, delay removal is a key factor in determining the accuracy of pulsar time.

Typically, the observed pulse arrival time (Δt) is corrected to the solar system barycenter. This correction depends on the pulsar's position, velocity, mass, and the solar system's celestial bodies. The equation for this correction can be summarized as:

$$\Delta t = \Delta c + \Delta_A + \Delta_{E\odot} + \Delta_{R\odot} + \Delta_{S\odot} - D/f^2 + \Delta_{VP} + \Delta_B$$

where Δc represents the Clock delay, Δ_A represents the Atmospheric delay, $\Delta_{E\odot}$ represents the Einstein delay, $\Delta_{R\odot}$ represents the Romer delay, $\Delta_{S\odot}$ represents the Shapiro delay, D/f^2 represents the Dispersion delay, Δ_{VP} represents the Parallax motion delay, Δ_B represents the Binary orbital motion delay.

For atmospheric delay, electromagnetic waves propagate more slowly through the atmosphere than in a vacuum. At typical observation frequencies, significant changes in total electron content can cause TOA fluctuations of 10 ns to several hundred ns (Liu, 2020).

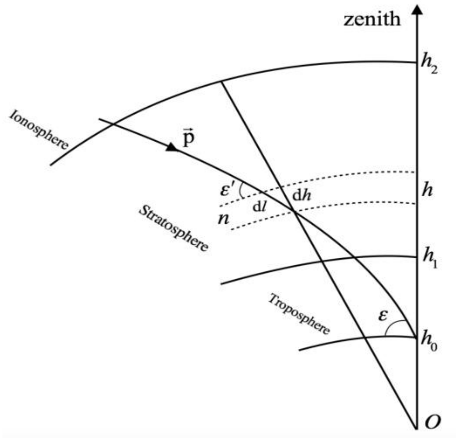

Figure 3: Atmospheric delay diagram (Liu, 2020)

Figure 3 is an illustration of atmospheric delay, where O represents the center of the Earth, and h_0 is the surface height of the Earth. The path of the electromagnetic wave is from h_0 to h_2, passing through different atmospheric layers: the stratosphere (between h_1 and h_2) and the troposphere (between h_0 and h_1). $\vec{P}$ is the path of an electromagnetic wave. The angle ε is the angle of elevation of the electromagnetic wave passing through the ionosphere, stratosphere, and troposphere until it reaches the ground-based telescope (Liu, 2020). The commonly used Saastamoinen (1972) model only considers the refractive time delay in the stratosphere and troposphere. The equation for the refractive delay is:

$$\Delta_A = \tau = \frac{1}{c}\int_{\vec{P}} \{n(l) - 1\} dl = \frac{1}{c}\int_{h_0}^{h_2} (n-1)\frac{dh}{\sin \varepsilon'}$$

Ignoring small corrections for latitude and height, the zenith delay is 7.69 ns, which is approximately 10 times the delay caused by water vapor. Atmospheric delay is related to the location of the ground-based telescope, and the mapping function is another important factor that determines atmospheric delay. The model by Herring (1992) is more suitable for separating dry and wet delays:

$$m(\varepsilon) = \frac{1 + \cfrac{a}{1 + \cfrac{b}{1+c}}}{\sin(\varepsilon) + \cfrac{a}{\sin(\varepsilon) + \cfrac{b}{\sin(\varepsilon) + c}}}$$

The refractive time delay is only effective for radio frequencies below 20 GHz.

This can help reduce dispersion effects and improve pulsar time accuracy for ultra-wideband and high-frequency observations. Atmospheric time delay requires better modeling, especially for observations with small elevation angles (10 degrees or less), where inaccuracies in the mapping function may significantly affect TOA (Time of Arrival) accuracy (Liu, 2020).

Please develop a model to solve the following problems:

Problem (1): Consider simulating the pulsar timing noise in Figure 2 with a functional model, aiming for a model fit of 95% or higher. The required data for modeling can be found in Attachment 1. The data relationships that can be referred to and not used include: the observed frequency of the pulsar is 1540 MHz in the radio band with a bandwidth of 320 MHz, the RMS value for MJD 52473 to 56081 is 75268.376 μs, and for MJD 52473 to 56646, the RMS value is 78502.322 μs. It is generally assumed that the intensity of red noise is proportional to the RMS value, though not equal.

Problem (2): Consider making short-term (ranging from a few days to one month) and long-term (ranging from several months to a few years) forecasts on the future trend of the pulsar timing noise in Figure 2, The required data for forecasting validation can be found in Attachment 1.

Problem (3): Consider modeling the refractive time delay for radio observation frequencies above 20 GHz, ensuring that the zenith delay is less than or equal to 7.69 ns. Relevant parameters and calculation processes can also refer to Chapter 6.1 of 《Space-Time Reference Systems》.

Problem (4): Consider modeling the atmospheric delay for observations with small elevation angles (10 degrees or less) to improve TOA accuracy. Please provide your model and also describe your considerations and the achievable goals.

References:

[1] Hobbs, G., Lyne, A. G., Kramer, M., An analysis of the timing irregularities for 366 pulsars[J]. 2010, MNRAS, 402(2):1027-1048.

[2] Matsakisd D N,Taylor J H,Eubanks T. A statistic for describing pulsasr and clock stabilities[J]. A&A,1997, 326: 924-928.

[3] Arzoumanian Z,Nice D J,Taylor J H, et al. Timing behavior of 96 radio pulsars[J]. 1994, 422(2): 671-680.

[4] 杨廷高,童明雷,高玉平.毫秒脉冲星计时噪声估计[J].时间频率学报,2014, 37(2): 80-88.

[5] Shannon R M,Cordes J M. Assessing the role of spin noise in the precision timing of millisecond pulsars[J]. 2010, ApJ,725(2): 1607-1619.

[6] Reardon D J,Hobbs G,Coles W,at al.Timing analysis for 20 millisecond pulsars in the parkes pulsar timing array[J]. 2016,MNRAS,455(2): 1751-1769.

[7] Huang N E, Shen Z, Long S R, et al. The empirical mode decomposition and the Hilbert spectrum for nonlinear and non-stationary time series analysis[J]. 1998,Mathematical, Physical and Engineering Sciences, 454(1971): 903-995.

[8] 高峰,高玉平,童明雷,等.经验模态分解方法在脉冲星计时残差分析及预报中的应用[J].天文学报,2018, 59(4): 3-13.

[9] 梁宏涛,刘硕,杜军威,等.深度学习应用于时序预测研究综述[J].计算机科学与与探索,2023,17(06):1285-1300.

[10] Kaspi V.M.,Taylor J.H.,Ryba M.F. High-Precision Timing of Millisecond Pulsars. III. Long-Term Monitoring of PSRs B1855+09 and B1937+21[J].1994,428:713.

[11] Liu Xiaojin. Pulsar Timing with the Next Generation of Radio Telescopes[D].2020,University of Manchester.

[12] Saastamoinen J. Contributions to the practical computation of astronomical refraction[J].Bull Geod 1972,106:383-397.

[13] Herring T., 1992, in DE Munck J. C., Spoelstra T. A. T., eds, Refraction of transatmospheric signals in geodesy. Nederlandse Commissie Voor Geodesie, Delft, pp 157–164.

[14] Niell A. E. Global mapping functions for the atmosphere delay at radio wavelengths [J].1996, Journal of Geophysics Research, 101, 3227-3246.

[15] Boehm J., Niell A., Tregoning P., Schuh H., Global Mapping Function (GMF): A new empirical mapping function based on numerical weather model data [J].2006a, Geophysics Research Letters, 33, L07304.

[16] Boehm J., Werl B., Schuh H., Troposphere mapping functions for GPS and very long baseline interferometry from European Centre for Medium-Range Weather Forecasts operational analysis data[J].2006b, Journal of Geophysical Research (Solid Earth), 111, B02406.

[17] Michael Soffel,Ralf Langhans 著,王若璞 赵东明译.时空参考系（Space-Time reference Systems）[D].北京.科学出版社，2015.8.